A Local Filtering Technique for Robot Skin Systems

Alessandro Albini[1], Giorgio Cannata[2] and Perla Maiolino[1]

***Abstract*— In this paper, we propose a local filtering technique directly applicable on large-area tactile sensing systems. The proposed filter can process the contact distribution without the need of intermediate steps that are required in the typical method of generating a tactile image. We particularly focus on the design of a filter to detect contours in the contact distribution. The approach is validated in a task of planar contour following performed using a robot equipped with two different end-effectors (planar and non-planar) sensorized with large-area tactile sensing technology. Additional experiments have been performed to evaluate strengths and limitations of the proposed approach with respect to tactile image-based data processing techniques.**

I. Introduction

Technological advancements have recently enabled the realization of complex large-area tactile systems, namely *robot skins*, composed of thousands of distributed transducers which can be conformed to curved surfaces and can potentially cover the whole robot body [1]–[5]. Despite the large number of tactile sensors technologies available, there is still a lack of standards at hardware level [6]. This makes it challenging to design tactile data processing algorithms that can be applied on such a large variety of devices.

Therefore, tactile data processing is usually performed by transforming raw sensor measurements into tactile images, i.e. planar representations of the contact pressure distribution [7]. The major limitation of tactile images is that they can only be directly generated from sensors distributed on a planar surface. Although it would still be possible to generate a tactile image from non-planar tactile sensors distributions [8], the procedure requires several processing steps and it can introduce distortions in the resulting tactile image.

The contribution of this paper is to present a technique to directly process the contact pressure distribution captured by a robot skin system without the need of intermediate steps required to generate tactile images. The proposed method is independent of the spatial arrangement of the tactile elements and the surface over which they are integrated. Within the scope of this paper, the specific problem of processing the contact distribution to extract contours is addressed.

Figure 1 illustrates the outcome of the proposed approach, where the contours of the contact distribution generated by two fingers pressing over a non-planar surface are correctly extracted. The proposed technique is validated in a task of planar contour following, where robot skin is integrated on two types of end-effectors: (i) a small flat end-effector with 20 tactile elements; (ii) a large and non-planar end-effector with 211 tactile elements. Furthermore, a comparison between the proposed method and an approach based on tactile images is presented, followed by an analysis of strengths and weaknesses of the proposed approach.

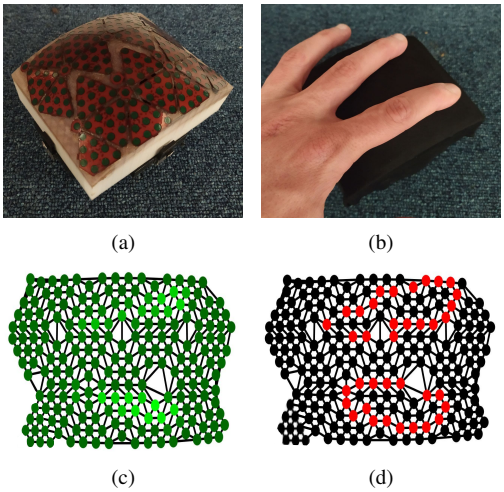

Fig. 1. The proposed method of edge detection filtering applied to a non-planar robot skin patch. (a) The CySkin technology integrated on a curved surface. Green circles correspond to independent pressure transducers. (b) A contact with two fingers. (c) Robot skin response (top view); darker dots correspond to lower responses. (d) Filtered robot skin response (top view).

II. Local Processing For Robot Skin

The robot skin system is composed of N distributed transducers, called *taxels*, mounted on a rigid non-planar manifold S with a non-regular spatial distribution. The position of each taxel $\mathbf{t}_i \in \Re^3$ is assumed to be known with respect to a given reference frame. We define $p(\mathbf{t}_i)$ the response of the robot skin system in the position $\mathbf{t}_i$. The taxel responses $p(\mathbf{t}_i)$, along with their positions in the space $\mathbf{t}_i$, provide a discrete information of the pressure distribution applied on S at a given time instant. The problem addressed in this paper is to introduce a filtering technique to compute the values $\hat{p}(\mathbf{t}_i)$, encoding contours in the pressure distribution.

Similarly to what proposed in [8], we represent taxels positions and their proximity relations by defining a *skin mesh*. In this representation, taxels are connected by edges (similarly to a graph structure) which provide both topological and geometric information. Let $T = \{\mathbf{t}_1, \ldots, \mathbf{t}_N\}$ be the set containing the position of each taxel. The Delaunay triangulation [9] applied to T allows to define a $N \times N$ matrix $\mathbf{E}$ describing topological relations among adjacent tactile

[1] are with the Oxford Robotics Institute (ORI), University of Oxford, UK.

[2] is with the Department of Informatics, Bioengineering, Robotics and Systems Engineering (DIBRIS), University of Genoa, Italy.

Corresponding author e-mail: alessandro@robots.ox.ac.uk

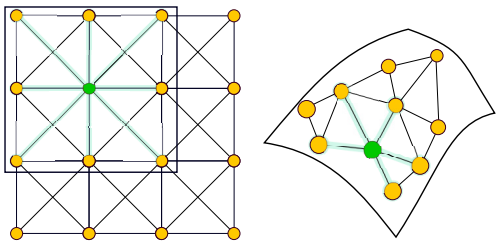

(a) (b)

Fig. 2. Adjacent taxels considered when computing Equation (3). (a) Taxels arranged as a flat 2D matrix. In this case Equation (3) corresponds to a convolutional operation performed with a 3×3 kernel mask. (b) Generic non-regular spatial arragement of taxels placed over a non-planar surface.

elements:

$$\mathbf{E} = [E]_{ij} = [E]_{ji} = \begin{cases} 1, & \text{if taxels } i \text{ and } j \text{ are connected} \\ 0, & \text{otherwise} \end{cases} \tag{1}$$

The set T containing taxel positions and the adjacency matrix $\mathbf{E}$ can be used to define a mesh $S^* = (T, \mathbf{E})$, representing a piecewise linear approximation of the sensorized surface S.

While T and $\mathbf{E}$ provide information on the topological connections among the taxels, the geometric relations, representing the distance among *connected* elements, can be represented with a matrix $\mathbf{D} \in \mathbb{R}^{N \times N}$, defined as:

$$\mathbf{D} = [D]_{ij} = [D]_{ji} = \|\mathbf{t}_i - \mathbf{t}_j\| E_{ij} \tag{2}$$

where $D_{ij} = 0$ for non-connected elements.

The information given by the adjacency matrix $\mathbf{E}$ can be used to compute the values $\hat{p}_i(\mathbf{t}_i)$ taking into account the response of nearby sensors. In this paper, the filtered values are computed as:

$$\hat{p}(\mathbf{t}_i) = p(\mathbf{t}_i) w_{ii} + \sum_{j \in \text{adj}(i)} p(\mathbf{t}_j) w_{ij} \tag{3}$$

where $w_{ij} \in \Re$ are scalar weight coefficients and $\text{adj}(i)$ is the adjacency list of the i-th taxel defined as:

$$\text{adj}(i) = \{j\} \ \forall j \in \{1, \ldots, N\} \ : \ E_{ij} = 1$$

Equation (3), representing a weighted sum of the taxel responses, can be rewritten in a more compact form by imposing $E_{ii} = 1$ for $i = \{1, \ldots N\}$. Therefore, Equation (3) becomes:

$$\hat{p}(\mathbf{t}_i) = \sum_{j \in \text{adj}(i)} p(\mathbf{t}_j) w_{ij} \tag{4}$$

It is worth noting that if taxels were arranged as a matrix (like pixels in an image) and w_{ij} were constants, Equation (4) would correspond to a 2D convolution operation performed with a 3x3 squared kernel (see Figure 2(a)). A graphical representation of Equation (4) applied to a generic skin mesh is represented in Figure 2(b). An Equation similar to (4) is used in Graph Convolutional Neural Networks to compute features in the hidden layers with w_{ij} learned at training time [10]. However, similarly to the image processing domain, it will be shown that a proper choice of the weights w_{ij} allows to design a filter. In this paper, they are computed to highlight edges in the pressure distribution, as described in the next Section.

III. Contour Extraction on Robot Skin Data

In image processing, contours can be detected in grayscale images by looking for variations in the luminance of nearby pixels. This is usually performed by designing convolutional masks approximating the first or second order derivative [11]. Due to the non-regular structure of the skin mesh, in this paper the weights w_{ij} are computed as an approximation of the *directional derivative* along the vector $\mathbf{k}_{ij} = \frac{\mathbf{t}_j - \mathbf{t}_i}{D_{ij}}$:

$$w_{ij} = \begin{cases} \frac{p(\mathbf{t}_i + D_{ij}\mathbf{k}_{ij}) - p(\mathbf{t}_i)}{D_{ij}}, & \text{if } i \neq j \\ 0, & \text{otherwise} \end{cases} \tag{5}$$

The weights computed with Equation (5) are not constant for each taxel. Indeed they depend on D_{ij} and $\mathbf{k}_{ij}$ that change when different set of taxels are considered. The weights in Equation (5) can be substituted in Equation (4), leading to:

$$\hat{p}(\mathbf{t}_i) = \sum_{j \in \text{adj}(i)} p(\mathbf{t}_j) \frac{p(\mathbf{t}_i + D_{ij}\mathbf{k}_{ij}) - p(\mathbf{t}_i)}{D_{ij}} \tag{6}$$

Therefore, $\hat{p}(\mathbf{t}_i)$ can be interpreted as the response to the input $p(\mathbf{t}_i)$ of a spatially varying linear filter. By computing Equation (6), even small variations on the intensity values among adjacent taxels are detected. Therefore, a tresholding operation must be performed on the values $\hat{p}_i(\mathbf{t}_i)$, thus obtaining:

$$\bar{p}(\mathbf{t}_i) = \begin{cases} 1, & \text{if } \hat{p}(\mathbf{t}_i) > \varepsilon \\ 0, & \text{otherwise} \end{cases} \tag{7}$$

where ε is a value that must be properly tuned to highlight edges in the contact shape. Figure 1 shows an example of the result of this filtering technique applied on human fingers pressing on a non-planar sensorized surface. As it can be seen, the values $\bar{p}_i(\mathbf{t}_i)$ mapped on the robot skin mesh allow to extract the contour of the fingers.

IV. Experimental Validation

The developed filter was validated in a simple task of planar contour following performed using a robot equipped with a sensorized end-effector. The tactile sensing technology used in this paper, namely CySkin, is presented in [12]. To validate the filtering technique proposed in this paper, CySkin was integrated on two different end-effectors (see Figure 3). The first is flat and contains 20 taxels. The second is non-planar and contains 221 taxels. Both end-effectors were fixed on a Franka Emika arm, which is used to perform the contour following task on two objects: a ruler (a straight line path) and a mug (a circular path). Figure 4 shows the objects and the non-planar end-effector in contact with them.

The proposed technique was compared with a tactile image based approach in the case of the non-planar end-effector. The processing pipeline needed to create a tactile image described in [8] was used. The tactile image is generated

(a) (b)

Fig. 3. The two end-effectors used to validate the proposed approach.(a) Planar tactile patch: 20 taxels.(b) Non-planar tactile patch: 211 taxels.

(a) (b)

Fig. 4. Object used to validate the proposed approach. (a) Robot following a ruler of 25 mm lenght and 1 mm thickness. (b) Robot following the contour of a mug of 81 mm and 75 mm outer and inner diameters respectively.

by resampling the flattened skin geometry with a step of 1 mm, generating an image of 74×132 pixels.

The experiments were performed using the following tapping-based procedure:

1) the robot starts from a random initial configuration where the end-effector is placed over the contour of the object that must be followed;
2) the robot proceeds with constant velocity along the z-axis until a contact is detected with tactile sensors;
3) the robot is controlled to apply a constant desired force along the z-axis of 15 N;
4) once the force controller reaches the steady state, the tactile measurements are filtered to extract the contours and the motion command is computed similarly to what described in [13];
5) the end-effector is lifted of 1 cm and its position and orientation are adjusted to be aligned with the contour of the object;
6) after the end-effector is correctly repositioned, the robot starts again from step (2) until the object contours are fully explored.

This procedure has been repeated three times for each object and end-effector.

V. Results and Discussions

Figure 5 reports the outcome of one of the three experiments of contour following performed on the mug in the case of the non-planar end-effector. Red dots correspond to the desired contact location $\mathbf{x}_R$ (see Figure 3) at each contact.

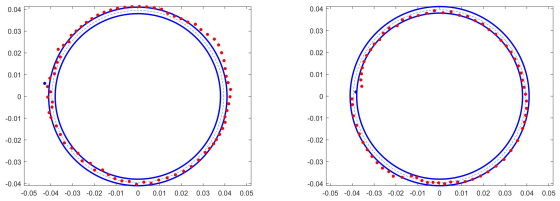

(a) (b)

Fig. 5. Example of circular contour reconstructed using the non-planar end-effector. Red dots correspond to the position of $\mathbf{x}_R$ at each contact. The blue lines represent the inner and outer perimeter of the mug. The blue dot corresponds to the initial position of $\mathbf{x}_R$. The exploration is performed clockwise. (a) Non-planar end-effector - proposed method. (b) Non-planar end-effector - tactile image based.

TABLE I

Results of the contour following task performed with the small planar end-effector.

Object	**Method**	$\bar{d}(mm)$	$\bar{\sigma}_d(mm)$	$d_M(mm)$
Ruler	Proposed approach	0.97	0.67	2.99
Ruler	Tactile Image	0.89	0.49	2.93
Mug	Proposed approach	1.53	0.87	4.16
Mug	Tactile Image	1.34	0.85	3.53

The blue dot represents the position of $\mathbf{x}_R$ at the first contact. The blue lines represent the inner and outer perimeter of the mug.

To evaluate whether the contours of the objects were correctly tracked, the position of $\mathbf{x}_R$ at each contact was recorded and the distance with the real contour of the object has been computed.

For each one of the three experiments the following statistics were computed: (i) the mean distance; (ii) the standard deviation; (iii) the maximum distance.

Tables I and II summarize the results obtained in all the three experiments reporting: $\bar{d}$ the average of the mean distances, $\bar{\sigma}$ the mean standard deviation and d_M the maximum distance across all the three experiments.

Results show that with both techniques the object contour is tracked with good accuracy. Indeed, the thickness of the ruler and the mug (respectively 1 mm and 3 mm) are lower than the pitch among the sensors, which is 7.5 mm. It can be seen from the Tables that the maximum error is much lower than the pitch. The method based on tactile images performs slightly better, providing a smoother reconstruction of the contour of the object. Indeed, the current limitation of the proposed method is that the contours extracted with Equation (4) exactly correspond to the positions $\mathbf{t}_i$. This in general is not true since the edge may pass through two adjacent taxels. This is clearly related to the resolution of the skin mesh. A finer pitch among the sensors would lead to more precise results. On the contrary, the filtering based on tactile images allows to reconstruct edges lying across the vertices composing the mesh. Indeed, with tactile image based methods the skin geometry is usually resampled using a grid with a finer resolution than the pitch among the sensors. This leads to a slightly higher precision in the

TABLE II

RESULTS OF THE CONTOUR FOLLOWING TASK PERFORMED WITH THE NON-PLANAR END-EFFECTOR.

Object	**Method**	$\bar{d}(mm)$	$\bar{\sigma}_d(mm)$	$d_M(mm)$
Ruler	Proposed approach	1.12	0.70	4.11
Ruler	Tactile Image	1.12	0.53	2.38
Mug	Proposed approach	1.86	0.96	5.21
Mug	Tactile Image	1.81	0.82	6.12

contour reconstruction. However, to overcome this limitation, we are currently evaluating the possibility of performing the same operation of resampling and interpolation directly on the 3D mesh, thus obtaining a finer mesh [14].

In terms of execution time, the proposed method is significantly faster. The computational time of the proposed method linearly scales with the number of vertices composing the mesh. Indeed, although Equation (4) requires the adjacency list, the maximum number of adjacent vertices is constant and fixed by the Delunay triangulation.
In the case of the curved patch, the code implementing Equation (4) takes an average of 0.075 ms to be executed for all taxels on a computer equipped with an Intel i7-10875H.

The computational time required to generate the tactile image linearly scales with the number of rows and columns. However, the execution time of the whole pipeline depends on the size of the contact area. Indeed, the pixels describing the contours (extracted from the tactile image) need to be back-projected on the skin mesh. The time required by this operation depends on how many pixels must be back-projected. In the case of the contour following, the method based on tactile images takes an average of 3.7 ms to be executed.

VI. CONCLUSION

In this paper a local filtering technique for robot skin data has been proposed. Differently from previous literature, where tactile images were used to process the contact shape, the proposed method can be directly applied even with a non-regular and non-planar arrangement of the tactile sensors, thus avoiding the use of additional processing steps needed to convert the tactile data to images. In particular, it has been shown how the proposed technique can be used to design a filter extracting sharp variations in the contact distribution. The filter was validated in a simple task of planar contour following, where the robot was commanded to follow a straight path and a circular one. As a possible extension of the work, several other filters can be designed to perform lowpass filtering or noise reduction, just to name but a few.

REFERENCES

[1] G. Cannata, M. Maggiali, G. Metta, and G. Sandini, "An embedded artificial skin for humanoid robots," in *2008 IEEE International Conference on Multisensor Fusion and Integration for Intelligent Systems*, Aug 2008, pp. 434–438.

[2] P. Mittendorfer and G. Cheng, "Humanoid multimodal tactile-sensing modules," *IEEE Transactions on Robotics*, vol. 27, no. 3, pp. 401–410, June 2011.

[3] Y. Ohmura, Y. Kuniyoshi, and A. Nagakubo, "Conformable and scalable tactile sensor skin for curved surfaces," in *Proceedings 2006 IEEE International Conference on Robotics and Automation, 2006. ICRA 2006.*, May 2006, pp. 1348–1353.

[4] D. S. Tawil, D. Rye, and M. Velonaki, "Improved image reconstruction for an eit-based sensitive skin with multiple internal electrodes," *IEEE Transactions on Robotics*, vol. 27, no. 3, pp. 425–435, June 2011.

[5] D. Um, B. Stankovic, K. Giles, T. Hammond, and V. Lumelsky, "A modularized sensitive skin for motion planning in uncertain environments," in *Proceedings. 1998 IEEE International Conference on Robotics and Automation (Cat. No.98CH36146)*, vol. 1, May 1998, pp. 7–12 vol.1.

[6] R. S. Dahiya, G. Metta, M. Valle, and G. Sandini, "Tactile sensing—from humans to humanoids," *IEEE Transactions on Robotics*, vol. 26, no. 1, pp. 1–20, 2010.

[7] S. Luo, J. Bimbo, R. Dahiya, and H. Liu, "Robotic tactile perception of object properties: A review," *Mechatronics*, vol. 48, pp. 54–67, 2017. [Online]. Available: https://www.sciencedirect.com/science/article/pii/S0957415817301575

[8] A. Albini and G. Cannata, "Pressure distribution classification and segmentation of human hands in contact with the robot body," *The International Journal of Robotics Research*, vol. 39, no. 6, pp. 668–687, 2020. [Online]. Available: https://doi.org/10.1177/0278364920907688

[9] J. E. Goodman and J. O'Rourke, Eds., *Handbook of Discrete and Computational Geometry*. USA: CRC Press, Inc., 1997.

[10] Z. Wu, S. Pan, F. Chen, G. Long, C. Zhang, and P. S. Yu, "A comprehensive survey on graph neural networks," *IEEE Transactions on Neural Networks and Learning Systems*, vol. 32, no. 1, pp. 4–24, 2021.

[11] R. Jain, R. Kasturi, and B. Schunck, *Machine Vision*, 01 1995.

[12] "Cyskin," https://www.cyskin.com/.

[13] L. Rocha, L. Velho, and P. de Carvalho, "Image moments-based structuring and tracking of objects." 01 2002, pp. 99–105.

[14] P. Alliez, G. Ucelli, C. Gotsman, and M. Attene, *Recent Advances in Remeshing of Surfaces*. Berlin, Heidelberg: Springer Berlin Heidelberg, 2008, pp. 53–82.